Resting-State Electroencephalographic Signatures Predict Treatment Efficacy of tACS for Refractory Auditory Hallucinations in Schizophrenic Patients

Xiaojuan Wang, Ruxin Hu, Tao Wang, Yuan Chang, Xiaoya Liu, Meijuan Li, Ying Gao, Shuang Liu, and Dong Ming, *Senior Member, IEEE*

***Abstract*—Transcranial alternating current stimulation (tACS) has been reported to treat refractory auditory hallucinations in schizophrenia. Despite diligent efforts, it is imperative to underscore that tACS does not uniformly demonstrate efficacy across all patients as with all treatments currently employed in clinical practice. The study aims to find biomarkers predicting individual responses to tACS, guiding treatment decisions, and preventing healthcare resource wastage. We divided 17 schizophrenic patients with refractory auditory hallucinations into responsive(RE) and non-responsive(NR) groups based on their auditory hallucination symptom reduction rates after one month of tACS treatment. The pre-treatment resting-state electroencephalogram(rsEEG) was recorded and then computed absolute power spectral density (PSD), Hjorth parameters (HPs, Hjorth activity (HA), Hjorth mobility (HM), and Hjorth complexity (HC) included) from different frequency bands to portray the brain oscillations. The results demonstrated that statistically significant differences localized within the high gamma frequency bands of the right brain hemisphere. Immediately, we input the significant dissociable features into popular machine learning algorithms, the Cascade Forward Neural Network achieved the best recognition accuracy of 93.87%. These findings preliminarily imply that high gamma oscillations in the right brain hemisphere may be the main influencing factor leading to different responses to tACS treatment, and incorporating rsEEG signatures could improve personalized decisions for integrating tACS in clinical treatment.**

***Index Terms*—Schizophrenia, refractory auditory hallucinations, resting-state electroencephalogram, transcranial alternating current stimulation, machine learning.**

I. Introduction

SCHIZOPHRENIA represents a severe psychiatric disorder primarily marked by positive symptoms, negative symptoms, and cognitive impairment, impacting approximately 1% of the global population [1]. One of the main positive symptoms of schizophrenia is hallucinations, which usually involve the patient perceiving sounds in the absence of external sound stimuli. The content of the voice is often accompanied by negative emotional valence, causing the patient to experience intense distress as well as severe dysfunction [2]. Overall, auditory hallucinations are reported in 60–80% of schizophrenic patients, which greatly raises the illness burden [3]. Thus, the treatment of auditory hallucinations is pivotal for schizophrenia.

The current approach to treating auditory hallucinations in schizophrenia appears to remain somewhat empirical, characterized by trial-and-error interventions [4]. Antipsychotic medications are commonly used in the clinical treatment of auditory hallucinations [5]. In fact, antipsychotic medications have minimal to no impact on roughly 30% of patients [6]. Currently, physical therapies have shown potential for alleviating the symptoms of auditory hallucinations [7], [8], [9], [10]. It is crucial to emphasize that irrespective of the therapeutic interventions employed, they are not effective for all patients. If certain patients exhibit an inadequate response to the initial treatment following a complete treatment cycle lasting approximately 2-4 weeks, it is advisable to contemplate a modification in the treatment regimen for subsequent therapeutic interventions [11]. It is not difficult to see that this is not only a waste of medical resources but also a delay in patients' conditions.

Received 17 January 2024; revised 15 April 2024, 15 June 2024, 15 September 2024, and 10 November 2024; accepted 27 November 2024. Date of publication 2 December 2024; date of current version 7 March 2025. This work was supported in part by the National Kev Research and Development Program of China under Grant 2023YFF1203700, and in part by the National Natural Science Foundation of China under Grant 62376187 and Grant 81925020. *(Xiaojuan Wang, Ruxin Hu, and Tao Wang contributed equally to this work.) (Corresponding author: Shuang Liu.)*

This work involved human subjects or animals in its research. Approval of all ethical and experimental procedures and protocols was granted by the Ethics Committee of Tianjin Anding Hospital (Tianjin Mental Health Center) under Application No. 2020-30, and performed in line with the ICH-GCP, China GCP, and relevant national regulations and laws.

Xiaojuan Wang, Tao Wang, Yuan Chang, Xiaoya Liu, Shuang Liu, and Dong Ming are with the Academy of Medical Engineering and Translational Medicine, Tianjin University, Tianjin 300072, China (e-mail: xiaojuanwang@tju.edu.cn; taowang2021@tju.edu.cn; 2022202108@tju.edu.cn; liuxiaoya@tju.edu.cn; shuangliu@tju.edu.cn; richardming@tju.edu.cn).

Ruxin Hu, Meijuan Li, and Ying Gao are with the Tianjin Anding Hospital, Mental Health Center of Tianjin Medical University, Tianjin 300070, China (e-mail: huruxin@tmu.edu.cn; meijuanli82@163.com; gaoying120225@163.com).

Digital Object Identifier 10.1109/JBHI.2024.3509438

Worth mentioning is that transcranial alternating current stimulation (tACS) is a promising complementary therapeutic option for refractory auditory hallucinations, and studies have shown significant changes in brain activity in patients after a period of intervention [12], [13]. tACS modulates cortical oscillations by applying sinusoidal alternating current to the scalp and selectively modulates oscillations at the applied frequency [14]. In this context, electroencephalography (EEG) emerges as a valuable tool in clinical applications for predicting the response to tACS, given its cost-effectiveness compared to magnetic resonance imaging (MRI) and has the potential to reveal specific frequency oscillations with high temporal resolution [15]. Functional near - infrared spectroscopy (fNIRS) studies on schizophrenia patients have revealed reduced hemodynamic activity, mainly in the prefrontal cortex, during cognitive tasks [16], [17], [18]. Joint studies employing fNIRS and EEG have demonstrated that both tACS and tDCS can augment brain oscillatory activity [19], [20], [21]. There have been reports that the fluctuations in δ, θ, α, β, and γ frequencies can reveal information about schizophrenia [22], [23]. Due to the fact that resting-state EEG (rsEEG) requires minimal cognitive effort, it has been extensively employed in schizophrenia investigations [24].

For rsEEG data analysis, Power spectral density (PSD) and Hjorth parameters (HPs), including Hjorth activity (HA), Hjorth mobility (HM), and Hjorth complexity (HC), are used to portray EEG signals in the frequency and time domain [25], [26]. PSD is a frequency signature of neural activity in the brain, with different frequency components corresponding to different types of EEG activity, reflecting the functional activity of the brain in different physiological states [27]. For HPs, HA reflects the overall level of neuronal activity in the brain. HM is used to describe the dynamics and rate of change of neuronal activity. HC reflects the level of complexity of neuronal activity, associated with more complex cognitive and information processing activities [26], [28], [29]. They provide better feature quality and higher classification stability [30]. Hence, prospectively determining the likelihood of treatment efficacy in patients can markedly mitigate treatment delays and facilitate tailored therapeutic interventions for distinct patient profiles.

In this study, our primary research goal is to find rsEEG features that accurately predict tACS responses in schizophrenic patients suffering from refractory auditory hallucinations. We categorized patients with auditory hallucinations into treatment responsive(RE) and non-responsive(NR) groups based on their auditory hallucination symptom reduction rates after one month of tACS treatment. For pre-treatment rsEEG, we extracted PSD and HPs(HA, HM, and HC included)across diverse frequency bands. Subsequently, these extracted features underwent rigorous statistical analysis across distinct brain regions delineated by anatomical localization. Finally, we input features with significant differences into multiple classifiers to verify their classification effects. At the same time, we expect that our work will help clinicians minimize the time wasted on useless treatments and promote the development of precision therapies.

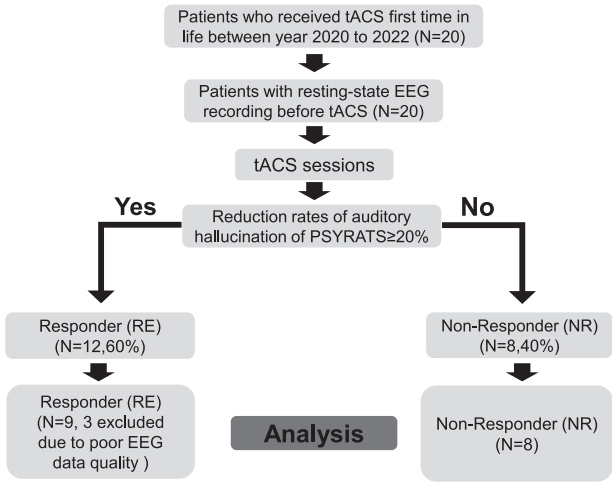

Fig. 1. Transcranial alternating current stimulation response diagram for refractory auditory hallucinations in schizophrenia.

II. Materials and Methods

A. Patients and Clinical Procedure

Seventeen participants, with an average age of 46.94 ± 13.56 (mean $\pm$ standard deviation) spanning the age range of 18 to 70, comprised the study cohort, featuring nine female participants. Each participant received a diagnosis of refractory auditory hallucinations through pre-treatment clinical assessment utilizing the Diagnostic and Statistical Manual of Mental Disorders, Fifth Edition (DSM-V). The Psychotic Symptom Rating Scales (PSYRATS) score was assessed both prior to the commencement of treatment and upon its completion. There is currently no standardized method for assessing the effectiveness of tACS treatment. According to our inclusion criteria, participants were enrolled who had a change in PSYRATS score of $\leq$20% or less in the fortnight preceding enrollment and who exhibited stable and significant hallucinatory symptoms. Taking the aforementioned into account, individuals experiencing a reduction of more than 20% in their auditory hallucination scores following one month of tACS intervention were categorized as responders to the tACS treatment (refer to Fig. 1). The study excluded individuals diagnosed with schizophrenia who had concurrent mental illnesses, substance abuse, suicide risk, head and neck implants, cardiac arrhythmia, pregnancy, seizures, epilepsy, and neurological disorders. Additionally, participants with a history of autoimmune disease, familial predisposition to immune disorders, and recent use of antibiotics and immunosuppressive drugs within the past four weeks were also excluded from the study. This study was approved by the Medical Ethics Committee of Tianjin Anding Hospital (2020-30).

B. Experimental Paradigm

Each participant underwent an 8-minute resting-state session, comprising eight 1-minute trials. During each 1-minute trial, participants were assigned to either the open-eye or closed-eye

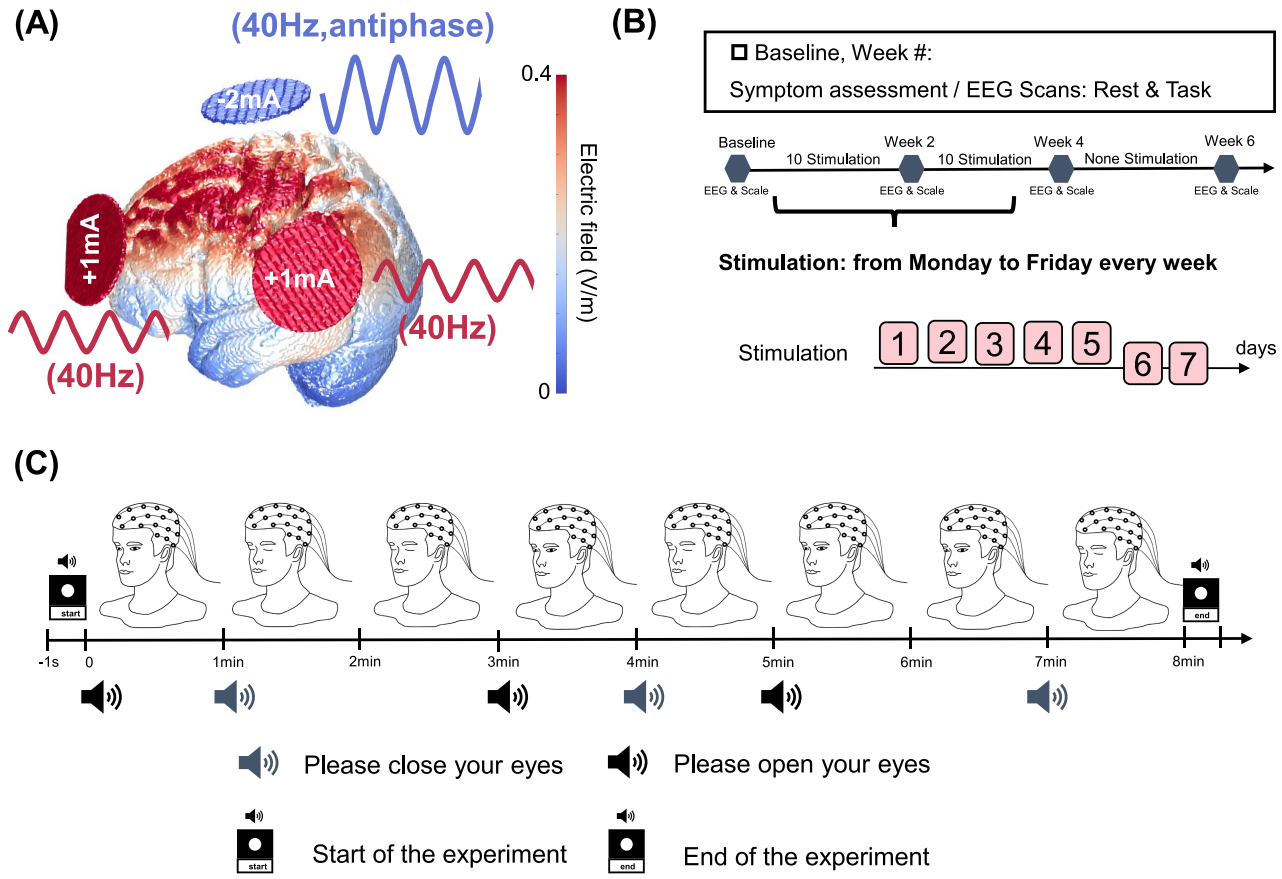

Fig. 2. (A) Schematic diagram of tACS. The figure shows that three stimulation channels were applied at AF3, CP5, and Cz(10-20 system). tACS at AF3 and CP5 (in-phase) has an amplitude of 1 mA (zero-to-peak), while the return current at Cz (reversed-phase) has an amplitude of −2 mA (zero-to-peak). (B) The procedure for the tACS intervention process: The EEG and PSYRATS scores were assessed at baseline (before the onset of electrical stimulation), during the stimulation process (Week 2 and Week 4), and at the follow-up session (Week 6). In this study, we use the baseline rsEEG to predict the week4 outcomes of auditory hallucinations. (C)The 8-min rsEEG paradigm. The sequence of whole eye closures is shown in the diagram.

condition, with the sequence alternating between open and closed eyes across the trials [31]. Specifically, the experimental paradigm employed in this study is depicted in Fig. 2(C), with four minutes dedicated to open-eye and four minutes to eyes-closed signals within the 8-minute resting-state session. During rsEEG recordings, an auditory stimulus is employed to prompt subjects to transition between open-eye and closed-eye states.

C. tACS Session Parameters

tACS was applied using the Starstim 32 (Neuroelectrics, Spain) in 10-20 electrode distribution. Regarding the parameter settings of tACS, our study was determined with reference to previous studies [13], [32]. The left dorsolateral prefrontal cortex (equal to AF3), temporal-parietal junction (equal to CP5), and central parietal lobe (equal to Cz) were applied the 1 mA, 1 mA, −2 mA altering current (zero-to-peak amplitude), respectively (See Fig. 2(A)). The electrode placement was determined through reference to our previous research [33] and previous research that employed tACS in the context of schizophrenia treatment [12]. Participants receiving tACS were administered 40 Hz alternating currents to the dorsolateral prefrontal cortex (dlPFC) and temporo-parietal junction(TPJ) electrodes in phase. Conversely, 40 Hz alternating currents at the return electrode were antiphase to those at the dlPFC and TPJ electrodes. The frequency of stimulation was 40 Hz with 20 minutes on weekdays for four consecutive weeks. Therefore, if a patient completes treatment, he or she will receive 20 sessions of stimulation (See Fig. 2(B)). For more detailed information, please refer to our previous article [34].

D. EEG Recording and Preprocessing

Uninterrupted EEG recordings were acquired using 64 Ag/AgCl electrodes positioned in accordance with the international 10–20 system. Interelectrode impedance was maintained below 10 kΩ . Data recording utilized a reference linked to the left mastoid electrode (M1), while the ground electrode was positioned at AFz. EEG data were digitized at a sampling rate of 1000 Hz, employing an online filter spanning 0.1–200 Hz.

The EEG data underwent preprocessing utilizing the EEGLAB toolbox and custom functions developed in MATLAB (MathWorks, Inc., Natick, MA, USA). First, electrodes that

were not utilized, including CB1, CB2, HEO, VEO, EKG, and EMG, were excluded from the experimental setup. The EEG data underwent down-sampling to 250 Hz and was re-referenced to the mean of the left and right mastoids. The function `pop_eegfiltnew.m` was utilized to apply a 0.5–120 Hz bandpass filter. To reduce interference from line noise, notch filters operating at 50 and 100 Hz were utilized. High-amplitude artifacts were automatically rejected by the EEGLAB plugin `clean_rawdata` using artifact subspace reconstruction [35]. The following parameters were employed: flat line removal for 10 seconds, electrode correlation threshold at 0.7, ASR at 100 (selected to account for the actual data quality), and window rejection set at 0.5. Spatial interpolation via spherical method was applied to handle rejected channels. Additionally, eye blinks, eye movement, muscle artifacts, and heartbeats were eliminated using independent component analysis (ICA). The EEGLAB plugin ICLabel [36] was utilized to choose brain ICs out of all other IC types. To rule out the effect of the eyes-closed condition on neural oscillations. Subsequently, 3 minutes artifact-free EEG epochs during open-eye conditions were randomly chosen for analysis. Any excess signal duration beyond 180 seconds for each subject was trimmed from the end of the EEG signal. This uniform signal length across all subjects aimed to mitigate potential bias in model performance attributable to subject-specific features.

E. Feature Extraction and Statistic

(1) **Welch FFT**: The PSD of the δ (1–4 Hz), θ (4–8 Hz), α (8–13 Hz), β (13–30 Hz), low-γ (30–50 Hz), and high-γ (50–100 Hz) bands [37] was calculated using Welch's FFT technique [38]. A data window is employed in each sequence to facilitate overlap [39], [40]. Let $xd(t)$ [41] represent the sequence, where $d = 1, 2, 3 \ldots L$ (signal intervals) and M denotes the interval length. Thus, the definition of power spectral density using the Welch method is as follows:

$$d(f) = \frac{1}{MU} \left| \sum_{t=0}^{M-1} xd(t)w(t)e^{-j2\pi f} \right|^2 \tag{1}$$

Here, U denotes the normalization factor for power in the window function.

$$U = \frac{1}{M} \sum_{t=0}^{M-1} |w(t)|^2 \tag{2}$$

The Welch power spectrum is computed as the average over modified periodograms, where $w(t)$ represents windowed data, and is defined by:

$$Welch(f) = \frac{1}{L} \sum_{i=0}^{L-1} d(f) \tag{3}$$

The MATLAB integrated function `pwelch.m` was employed for PSD estimation. In this investigation, 3-minute open-eye EEG signals were partitioned into 4-second segments with no overlap [42], resulting in 45 equal segments. Each segment was subjected to the Hamming window, and the resulting periodograms were averaged to determine the PSD estimate.

(2) **Hjorth activity, mobility, and complexity (HA, HM, and HC)**: Hjorth defined three parameters, namely activity, mobility, and complexity, to summarize EEG signals in the time domain [43]. Activity is computed as the signal's standard deviation. The mobility parameter is formulated as the square root of the standard deviation of the first derivative of the signal divided by the standard deviation of the signal. Hjorth complexity is determined by the ratio of the mobility of the first derivative of the signal to the mobility of the signal, thereby serving as an index of signal complexity. Lastly, the amplitude, time scale, and complexity of the EEG signal are all described by these three parameters, respectively. Equations (4), (5), and (6) were utilized to obtain HA, HM, and HC, where $Var(x(t))$ is the variance of the signal $x(t)$ and $\frac{dx(t)}{dt}$ is the first derivative of the signal $x(t)$.

$$HA = Var(x(t)) \tag{4}$$

$$HM = \sqrt{\frac{Var\left(\frac{dx(t)}{dt}\right)}{Var(x(t))}} \tag{5}$$

$$HC = \frac{HM\left(\frac{dx(t)}{dt}\right)}{HM(x(t))} \tag{6}$$

Before the calculation, the EEG signal is filtered by the `eegfilt.m` function according to the frequency bands mentioned above, and HA, HM, and HC are calculated for different frequency bands. To be consistent with the length of the data calculating the power spectral density, we cut the 3 minutes long EEG signals into 4 s segments. To compute the three metrics from our EEG data, we utilized the MATLAB code that de Miras had used [44].

To assess disparities in the extracted features between the two groups across different brain regions, eight regions of interest (ROIs) are defined based on their anatomical locations [45]. The distribution of brain regions is shown schematically in Fig. 3(A) (green: left frontal lobe(LF), right frontal lobe(RF), blue: left temporal lobe (LT), right temporal lobe (RT),pink: left parietal lobe (LP), right parietal lobe (RP),orange: left occipital lobe (LO),right occipital lobe (RO)). Custom R scripts were employed for the statistical analysis of demographic and EEG data. Conducting independent sample t-tests, group comparisons were performed, with the exception of gender, family history, Clozapine, and antipsychotic drug (APD) use, which were evaluated using a Chi-square test. Furthermore, a rank-sum test was applied for comparing EEG features between the two groups. The raw p-values were subjected to false discovery rate (FDR) correction in order to reduce the quantity of false-positive errors brought on by multiple comparisons [46].

F. Classification

In this section, based on the results of the above statistical analysis, we explore the predictive ability of rsEEG features for tACS response in refractory auditory hallucinations using the above features with significant differences. Time-domain features (HA, HM, and HC), frequency-domain features (PSD),

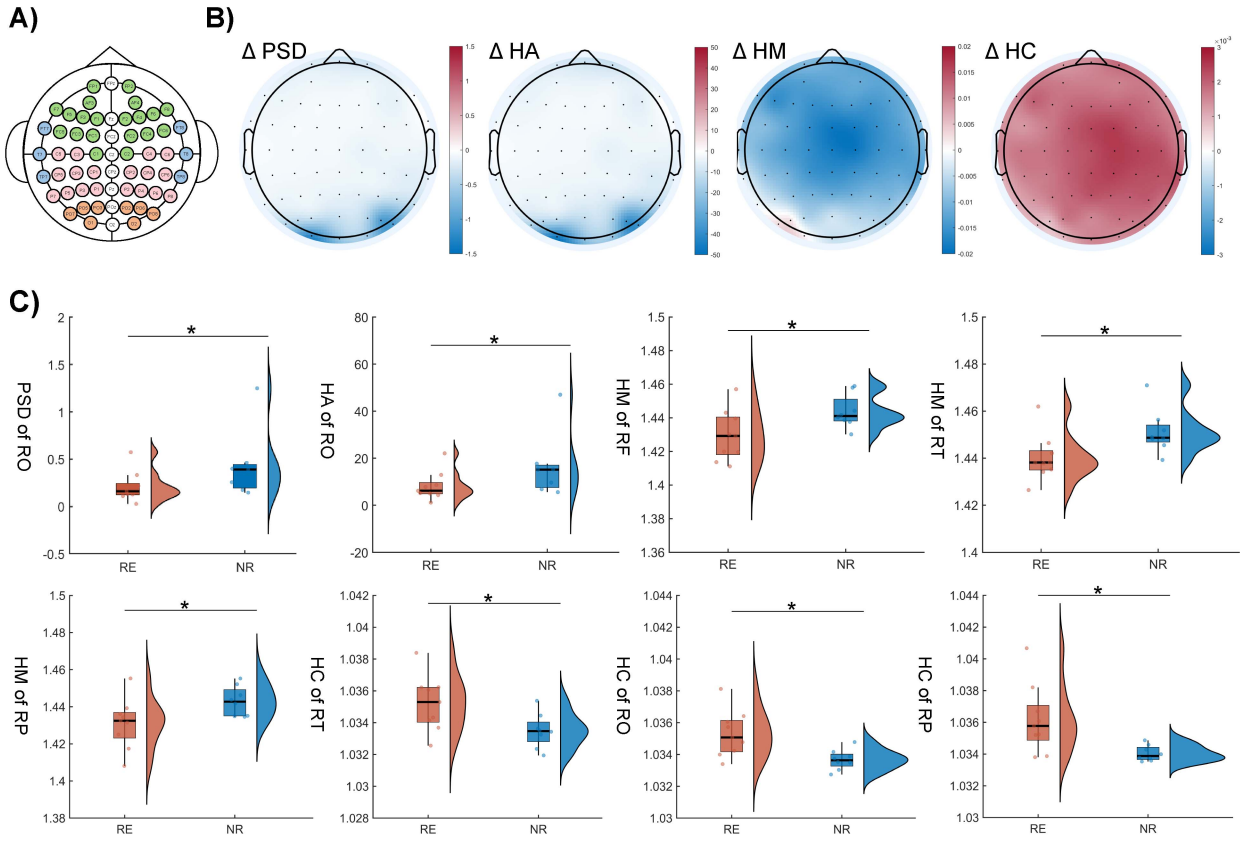

Fig. 3. EEG time and frequency domain features of high gamma frequency bands. (A) Schematic diagram of the division of brain regions. (green: left frontal lobe(LF), right frontal lobe(RF), blue: left temporal lobe (LT), right temporal lobe (RT),pink: left parietal lobe (LP), right parietal lobe (RP),orange: left occipital lobe (LO),right occipital lobe (RO),white: middle line). (B) Whole-brain differences in time- and frequency-domain features. (Δ : responders $-$ non-responders). (C) Salient features of different brain regions in the high-γ (50–100 Hz) band. ($* : p < 0.05$).RE indicates a response, while NR indicates no response.

and time-frequency fusion features (HA, HM, HC, and PSD) were utilized separately to obtain the optimal EEG feature patterns for predicting tACS responses, thereby improving the performance and robustness of the predictive model. In this paper, eight common classifiers were used to classify tACS responses.

For time-frequency feature fusion, we first define the feature extraction function:

$$X_{\mathrm{R,T}} = ExtractFeatures(R, T, D) \tag{7}$$

Here, $X_{(R,T)}$ denotes multiple features extracted from different sets of brain regions R against the feature set T, and D represents the input brain region data. $T = \{\mathrm{PSD}, \mathrm{HA}, \mathrm{HM}, \mathrm{HC}\}$, $R = \{\mathrm{RF}, \mathrm{RT}, \mathrm{RP}, \mathrm{RO}, \mathrm{LF}, \mathrm{LT}, \mathrm{LP}, \mathrm{LO}\}$. Next, for each feature vector, we assessed its significant difference across conditions by statistical tests:

$$p_{(\mathrm{R,T})} = StatTest(X_{\mathrm{R,T}}) \tag{8}$$

Here, $p_{(R,T)}$ is the significance p-value of the eigenvector $X_{(R,T)}$ under a given statistical test.

$$S = \bigcup_{\substack{R \in R \\ T \in T}} \{x_{(R,T)} \mid p_{(R,T)} < \alpha\}$$

$$\begin{aligned} &= [(RO, \mathrm{PSD}), (RO, \mathrm{HA}), \\ &\quad (RF, \mathrm{HM}), (RT, \mathrm{HM}), (RP, \mathrm{HM}), \\ &\quad (RT, \mathrm{HC}), (RP, \mathrm{HC}), (RO, \mathrm{HC})] \end{aligned} \tag{9}$$

Here, $\bigcup$ denotes the concatenation operation on the set of features, and α is a predetermined level of significance ($\alpha = 0.05$). S is a sequence that defines the features with significant differences in the brain regions where they are located. Finally, we splice the filtered features to form the final fused feature vector F:

$$F = \bigoplus_{(r,t) \in S} X_{(R,T)} \tag{10}$$

To evaluate the prediction performance of the extracted EEG features for tACS response in individuals with schizophrenia, four machine learning models and four deep neural network models were used in this study, including Support Vector Machine (SVM), K-Nearest Neighbors (KNN), Random Forest (RF), Linear Discriminant Analysis (LDA), Multilayer Neural Network (MNN), Recurrent Neural Network (RNN), Feedforward Neural Network (FNN), and Cascade Forward Neural Network (CFNN). Some of these models have been successfully applied to EEG-based recognition tasks [47], [48], [49], [50]. We used

TABLE I
ARCHITECTURES AND CONFIGURATIONS OF FOUR NEURAL NETWORKS

Network	Hidden layers	Hidden neurons	Output
MNN	4	[8, 8, 16, 16]	2
RNN	4	[8, 8, 16, 16]	2
FNN	4	[8, 8, 16, 16]	2
CFNN	4	[8, 8, 16, 16]	2

the SVM classifier with linear kernel, which was implemented by the LIBSVM toolbox [51] using default parameters. For the KNN classifier, the Euclidean distance was selected as a distance metric, and the number of nearest neighbors was set to six. The RF was implemented using the RandomForest-MATLAB function [52], and the number of trees (ntree) was set to 500. The LDA was modeled with default parameters. The network structures of the four neural networks are detailed in Table I. The training algorithm for the MNN employed the scaled conjugate gradient (CG) method [53], and the performance was assessed using cross-entropy. For the RNN, FNN, and CFNN, we employed the Levenberg-Marquardt (LM) training algorithm [53], and the performance was evaluated using the mean squared error (MSE).

To prevent ignoring important features with small values during model training, the min-max normalization method was used to normalize the features into [0, 1] before performing the classification [54]. All the experiments were performed using the 10-fold cross-validation method, and the accuracy, sensitivity, specificity, F1-score, and area under the curve (AUC) of the receiver operating characteristic (ROC) were used to evaluate the experimental performance. Sensitivity refers to the testing accuracy in individuals who respond to tACS stimulation, and specificity refers to the testing accuracy in individuals who do not respond to tACS stimulation.

III. RESULTS

A. Participants Characteristics

After preprocessing, the quality of open-eye rsEEG data from three subjects in the responder group was so poor and they were not included in this analysis. Table II summarizes the demographic and clinical characteristics of the participants. The results show that there was no difference in gender, age, education, duration of disorder, medication use and clinical symptom scores between tACS responders and non-responders.

B. EEG Features Results

We statistically analyzed the EEG features in all frequency bands in the eyes-open state, and ended up finding significant differences only in the high gamma band. The PSD and HPs were computed for responders and non-responders, Fig. 3(B) shows the difference between two groups within high gamma frequency bands. Obviously, the resemblance in differences between PSD and HA, suggesting a potential overlap of information conveyed by these two features across both frequency and time domains. Conversely, the distinctions observed in HM and HC were distributed widely across the brain. Furthermore, the discrepancies between HM and HA were entirely contradictory, indicating that these two features may represent distinct aspects within the time domain.

Further, the calculated PSD and HPs of the two groups were subjected to independent samples t-test according to the distribution of brain regions. As shown in Fig. 3(C), the results showed that the responder group had significantly lower PSD and HA values of high gamma in the right occipital region than the non-responders ($z = -2.07, p_{\text{fdr}} = 0.04$). This indicated that high-frequency neural oscillatory activity in the right occipital lobe region was insufficient in the responder group. In addition, comparing to non-responders, responders had significantly lower HM values in the frontal ($z = -2.07, p_{\text{fdr}} = 0.04$), temporal ($z = -2.45, p_{\text{fdr}} = 0.01$), and parietal lobes ($z = -2.07, p_{\text{fdr}} = 0.04$), indicating that the EEG signals of non-responders change relatively quickly and are not stable enough in time scale. But responders had significantly higher HC values in the temporal ($z = 2.17, p_{\text{fdr}} = 0.03$), parietal ($z = 2.65, p_{\text{fdr}} = 0.01$), and occipital lobes ($z = 2.45, p_{\text{fdr}} = 0.01$), indicating that the EEG signals in these brain areas of responders are more complex. All in all, both responders and non-responders had significant differences in EEG features in the high gamma frequency band of the right hemisphere, suggesting that the effects of tACS may be well represented by high-frequency neural oscillatory activity in the right hemisphere of the brain.

C. Classification Results

Table III presents the classification performance of time-domain features, frequency-domain features, and time-frequency fusion features across multiple classifiers. As shown in Table III, for the time-domain features, the best accuracy of 91.21% was achieved by the CFNN. For the frequency-domain features, the best accuracy of 82.55% was achieved by the FFNN. The time-frequency fusion feature achieved the highest classification accuracy of 93.87% in the CFNN classifier, which significantly outperformed the individual time- or frequency-domain features. Furthermore, except for MNN, the time-frequency fusion features obtained the optimal results for all evaluative metrics in all classifiers, outperforming the individual time-domain features and frequency-domain features. These results indicate that the fusion of time and frequency-domain features enhances the robustness and discriminative ability of rsEEG features for predicting tACS response in schizophrenic patients with refractory auditory hallucinations.

As shown in Table III, the classifier with the best results in the time-domain features and fusion features is CFNN, and the best performance in the frequency domain features is FFNN, both of which are neural network models. In addition, the extracted time-frequency fusion features are low-dimensional features, and the sample size of this research is small, which indicates that the proposed fusion features are more suitable for modeling with neural networks. They effectively alleviate the overfitting problem of deep neural networks for small samples and low-dimensional features and are more suitable for the

TABLE II
DEMOGRAPHIC AND CLINICAL PROFILES OF INDIVIDUALS DIAGNOSED WITH SCHIZOPHRENIA AND REFRACTORY AUDITORY HALLUCINATIONS WHO UNDERWENT A TRANSCRANIAL ALTERNATING CURRENT STIMULATION INTERVENTION

Measure	**Non-Responder (n=8)** (mean ± sd)	**Responders (n=9)** (mean ± sd)	**t/x^2**	***P*-value**
Demographics				
Age(years)	46.50 ± 15.71	47.33 ± 12.30	-0.12	0.91
Education (years)	11.25 ± 2.55	11.44 ± 3.43	-0.13	0.90
Duration (years)	21.25 ± 14.81	18.22 ± 11.40	0.47	0.65
Eqdose (mg)	420.00 ± 177.14	500.00 ± 206.53	-0.86	0.40
Gender (Male)	3/5	6/3	0.51	0.47
Family history (y/n)	1/7	1/8	0.00	1.00
Clozapine(y/n)	4/4	5/4	0.00	1.00
APD (y/n)	3/5	6/3	0.51	0.47
Baseline Measures				
PANSS				
Hallucinations	6.12 ± 0.64	5.89 ± 0.60	0.78	0.45
Total score	89.00 ± 23.77	88.78 ± 13.56	0.02	0.98
Positive Symptoms	25.50 ± 3.70	25.00 ± 4.15	0.26	0.80
Negative Symptoms	24.62 ± 10.47	28.22 ± 4.35	-0.90	0.39
General psychopathology	38.88 ± 10.79	35.56 ± 7.94	0.71	0.49
PSYRATS				
Total Score	53.25 ± 7.29	53.89 ± 9.12	-0.16	0.88
Auditory hallucinations	34.00 ± 5.07	35.67 ± 4.82	-0.69	0.50
Delusions	19.25 ± 3.58	18.22 ± 5.17	0.48	0.64

TABLE III
THE CLASSIFICATION OUTCOMES OF TIME-DOMAIN, FREQUENCY-DOMAIN, AND TIME-FREQUENCY FUSION FEATURES ACROSS DIVERSE EVALUATION METRICS (ACCURACY, SENSITIVITY, SPECIFICITY, F1-SCORE, AND AUC)

Feature	Classifier	Accuracy	Sensitivity	Specificity	F1-score	AUC
Time Domain Features	SVM	0.8441	0.8916	0.7907	0.8583	0.9126
	KNN	0.8784	0.9086	0.8444	0.8878	0.9409
	RF	0.8752	0.8556	0.8972	0.8789	0.9502
	LDA	0.7679	0.8872	0.6338	0.8019	0.8613
	MNN	0.9075	**0.9491**	0.8608	0.9157	**0.9633**
	RNN	0.8895	0.8833	0.8965	0.8944	0.9521
	FFNN	0.9010	0.8963	0.9063	0.9055	0.9600
	CFNN	**0.9121**	0.9130	**0.9111**	**0.9166**	0.9619
Frequency Domain Features	SVM	0.7398	**0.8559**	0.6091	0.7769	0.8184
	KNN	0.7493	0.8364	0.6514	0.7794	0.8214
	RF	0.7954	0.8012	0.7889	0.8057	0.8903
	LDA	0.6834	0.7809	0.5738	0.7231	0.7779
	MNN	0.7792	0.7825	0.7756	0.7896	0.8687
	RNN	0.7931	0.8017	0.7833	0.8040	0.8726
	FFNN	**0.8255**	0.8321	**0.8181**	**0.8347**	**0.9119**
	CFNN	0.8134	0.8340	0.7903	0.8255	0.9045
Fusion Features	SVM	0.9049	0.9241	0.8832	0.9114	0.9603
	KNN	0.8837	0.9037	0.8611	0.8916	0.9448
	RF	0.9129	0.9066	0.9199	0.9168	0.9746
	LDA	0.8692	0.9335	0.7969	0.8831	0.9443
	MNN	0.9055	0.9055	0.9056	0.9103	0.9662
	RNN	0.9203	0.9136	0.9278	0.9238	0.9662
	FFNN	0.9301	0.9395	0.9194	0.9343	0.9698
	CFNN	**0.9387**	**0.9395**	**0.9378**	**0.9420**	**0.9771**

The optimal results in this table are highlighted in bold.

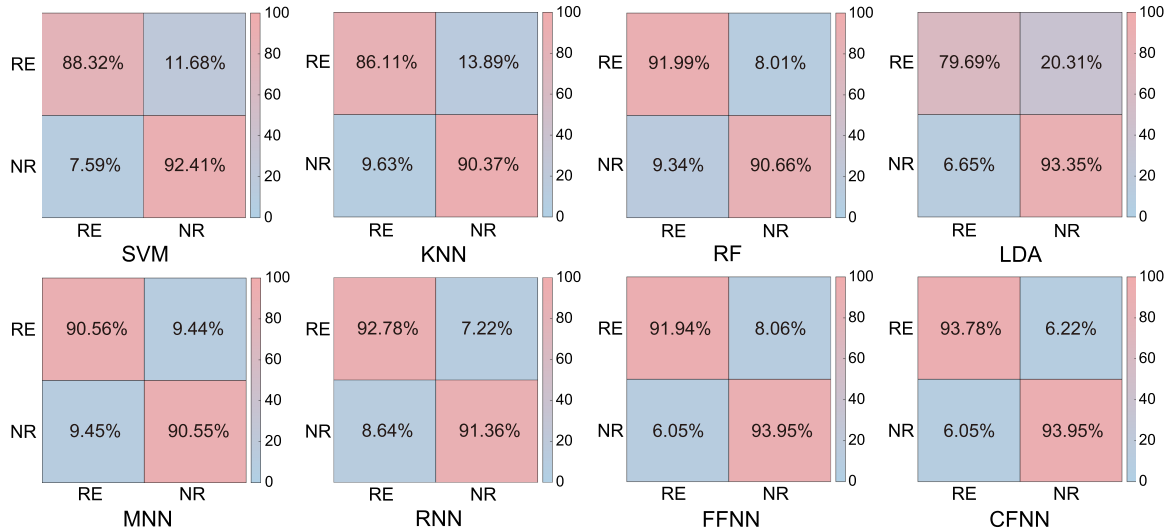

Fig. 4. The confusion matrix for tACS response recognition of the proposed time-frequency fusion features on various classification models. RE indicates a response, while NR indicates no response.

task of predicting individual tACS responses in schizophrenic patients with refractory auditory hallucinations.

In Fig. 4, the recognition outcomes of the suggested time-frequency fusion features are depicted through a confusion matrix encompassing eight classification models. Each row in the matrix corresponds to a ground truth class, while each column represents a predicted class. As presented in Fig. 4, the proposed fusion feature performs well in all neural networks in the task of identifying tACS responses, achieving more than 90% accuracy for response or no response. Moreover, although the performance of fused features in four classic machine learning models is weaker than that of neural networks, they still achieved more than 85% accuracy. These results show that the proposed time-frequency fusion feature achieves excellent recognition performance in a variety of classical classifiers, further demonstrating the discrimination and generalization of the proposed fusion features in the task of predicting tACS responses in schizophrenic patients.

The AUC is recognized for its efficacy in assessing the performance of binary classification models [55], therefore, we employ it to assess the discriminative ability of the models. Fig. 5 presents the ROC curve of the proposed time-frequency fusion features across eight classifiers. As shown in Fig. 5, the AUC values of the fused features reached more than 94% in all eight classifiers, indicating the good robustness and stability of our method. Overall, our method achieved good classification results for predicting tACS responses in schizophrenia patients by fusing EEG multi-dimensional features in the time and frequency domains and achieved good generalization results on a number of different classifiers.

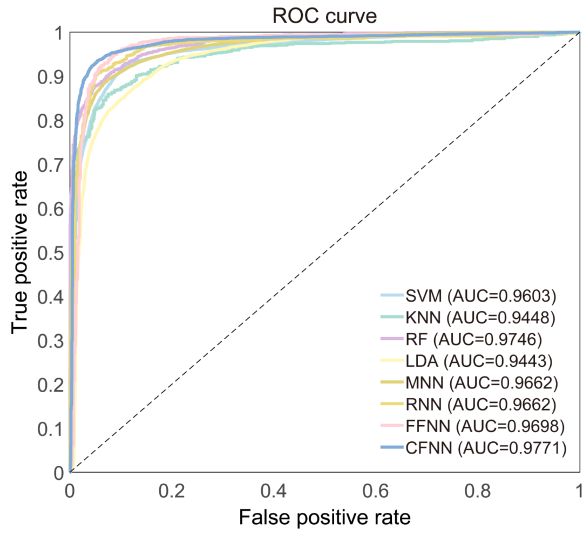

Fig. 5. The ROC curves of the proposed time-frequency fusion features on eight recognition models.

IV. Discussion

This study represents the pioneering utilization of machine learning analysis on fused time-frequency domain features of rsEEG to predict individual responses to tACS in refractory auditory hallucinations of schizophrenia. Both time and frequency-domain features of responders and non-responders differed significantly in the high gamma frequency band of the right brain hemisphere, suggesting that high-frequency EEG activity in the right brain hemisphere may influence an individual response to tACS. In the predictive model, the dissociable features of the right cerebral hemisphere hold notable accuracy, sensitivity, specificity, F1-score, and AUC in distinguishing responders from non-responders to tACS. In addition, the time-frequency fusion features can achieve better classification results on different classifiers, and the AUC values of the eight typical classifiers reach more than 94%. These findings preliminarily indicate that time-frequency domain fusion features extracted from pre-treatment rsEEG can function as a reliable predictor

of tACS responses in individuals diagnosed with schizophrenia experiencing refractory hallucinations.

The etiology and pathophysiology of auditory hallucinations, the most common positive symptom of schizophrenia, are unknown [41], [56], [57]. Most contemporary research links auditory hallucinations to increased activity in the auditory cortex of the left temporo-parietal junction, reduced activity in the left dorsolateral prefrontal cortex, and decreased functional connectivity within the left frontal-temporal-parietal network [58], [59], [60], [61], [62]. This study revealed a significant correlation between the synchronization of gamma oscillations in the left auditory cortex of patients and the manifestation of auditory hallucinations symptoms [63], [64], [65]. **Additionally, analysis of the patients revealed that the correlation dimension in the gamma frequency band was higher in the right prefrontal cortex of those with auditory hallucinations compared to those without [66].** Based on these findings, differences in the right hemisphere of the brain will be magnified in comparative analyses of schizophrenic patients who also suffer from auditory hallucinations and are refractory to treatment. This is also consistent with our current findings. Dissimilarities in rsEEG attributes between individuals responding and not responding to treatment were predominantly observed within the high gamma frequency range of the right cerebral hemisphere. Therefore, right hemisphere deficits also play a very important role in schizophrenic patients [67].

tACS has shown great potential in the treatment of hallucinatory symptoms in schizophrenia. Therefore, understanding whether patients can benefit from tACS treatment is valuable for both physicians and patients. Pre-treatment rsEEG time-frequency fusion features were selected in this study to accurately predict responses to tACS in patients with refractory auditory hallucinations. In terms of predicting individual responses, Beomjun et al. achieved a prediction accuracy of 85.2% by using transfer entropy of rsEEG in order to make predictions of response to electroconvulsive therapy in patients suffering from schizophrenia [68]. Ronny et al. predicted individual responses to ECT in septuagenarian patients by analyzing individual structural magnetic resonance data with accuracy rates of 78.3% and sensitivity rates of 100% [69]. Cao et al. presented a clinical instrument capable of forecasting the response to risperidone treatment in first-episode drug-naive patients with schizophrenia, achieving a balanced accuracy rate of 82.5% [70]. Not surprisingly, current neuroimaging methods report correct classification rates between 70% and 85%. Our study shows that the classification accuracy of time-frequency domain fusion features on the CFNN model is as high as 93.8%, and the extracted time-frequency fusion features belong to the low-dimensional features, indicating that it overcomes the overfitting problem of the deep learning network for the small samples with low-dimensional features and is more suitable for tACS treatment applications.

This study has several limitations. Primarily, it is worth noting that our study entailed the prediction of individual responses to tACS in the context of drug-combined tACS rather than solely tACS. This distinction arises from the fact that all patients received medication concurrent with the tACS intervention, and no notable dissimilarity existed in terms of equivalent drug dosages between the two groups. Nonetheless, we cautiously assumed minimal drug-related interference with the outcomes. However, it remains pertinent to acknowledge the varying effects of different medications on patients' neural oscillatory activity. Consequently, future investigations should exercise stringent control over the influence of pharmaceutical agents in such studies. Secondly, it is essential to consider that our study transpired during the backdrop of the COVID-19 pandemic, a period that posed substantial challenges to the overall subject recruitment for our experimental cohort. Consequently, the final count of patients who successfully concluded the intervention was relatively modest. We also segment the data to compensate to some extent for the small sample size. Lastly, it is worth noting that our classification of responders and non-responders did not strictly align with the prevailing consensus in assessing medication effects. Instead, we relied on the criteria specified in the inclusion criteria, which required a minimum 20% reduction in auditory hallucinations symptom scores on the PSYRATS scale. Given that our study exclusively encompassed individuals with schizophrenia afflicted by refractory auditory hallucinations, we contend that this criterion for dichotomization remains scientifically justified. Subsequent investigations ought to rigorously address these confounding factors and expand upon the present findings, striving to furnish a comprehensive elucidation of the underlying mechanisms governing the tACS response in individuals afflicted with refractory hallucinations within the context of schizophrenia.

V. Conclusion

In summary, the present study preliminarily provides evidence using rsEEG time-frequency fusion features to predict the response to tACS in individuals with schizophrenia who suffer from refractory auditory hallucinations. The proposed time-frequency fusion feature of the right brain region was demonstrated to have good discriminative and generalization performance in predicting tACS responses, and it obtained the highest recognition accuracy of 93.87% achieved by the CFNN. While rigorous long-term investigations are warranted to achieve precise individual patient response prediction in a clinical context, the utilization of rsEEG assessment before formulating treatment plans emerges as an objective, straightforward, and cost-effective approach, facilitating clinicians in rendering judicious therapeutic decisions. Future research on biomarkers that predict response to tACS is expected to reduce wasted resources, prevent delays in optimal treatment, and significantly advance precision medicine in clinical practice.

References

[1] R. A. McCutcheon, T. R. Marques, and O. D. Howes, "Schizophrenia—an overview," *JAMA Psychiatry*, vol. 77, no. 2, pp. 201–210, 2020.

[2] S. McCarthy-Jones et al., "Better than mermaids and stray dogs? subtyping auditory verbal hallucinations and its implications for research and practice," *Schizophrenia Bull.*, vol. 40, no. Suppl_4, pp. S275–S284, 2014.

[3] A. Lim et al., "Prevalence and classification of hallucinations in multiple sensory modalities in schizophrenia spectrum disorders," *Schizophrenia Res.*, vol. 176, no. 2/3, pp. 493–499, 2016.

[4] A. Kruger, "Schizophrenia: Recovery and hope," *Psychiatr. Rehabil. J.*, vol. 24, no. 1, pp. 29–37, 2000.

[5] Y. Hirano and S. Tamura, "Recent findings on neurofeedback training for auditory hallucinations in schizophrenia," *Curr. Opin. Psychiatry*, vol. 34, no. 3, pp. 245–252, 2021.

[6] J. M. Kane, T. Kishimoto, and C. U. Correll, "Non-adherence to medication in patients with psychotic disorders: Epidemiology, contributing factors and management strategies," *World Psychiatry*, vol. 12, no. 3, pp. 216–226, 2013.

[7] J. M. Mellin et al., "Randomized trial of transcranial alternating current stimulation for treatment of auditory hallucinations in schizophrenia," *Eur. Psychiatry*, vol. 51, pp. 25–33, 2018.

[8] R. B. Force, J. Riddle, L. F. Jarskog, and F. Fröhlich, "A case study of the feasibility of weekly tACS for the treatment of auditory hallucinations in schizophrenia," *Brain Stimul., Basic, Transl., Clin. Res. Neuromodulation*, vol. 14, no. 2, pp. 361–363, 2021.

[9] A. Vercammen et al., "Effects of bilateral repetitive transcranial magnetic stimulation on treatment resistant auditory–verbal hallucinations in schizophrenia: A randomized controlled trial," *Schizophrenia Res.*, vol. 114, no. 1–3, pp. 172–179, 2009.

[10] F. Fröhlich et al., "Exploratory study of once-daily transcranial direct current stimulation (tDCS) as a treatment for auditory hallucinations in schizophrenia," *Eur. Psychiatry*, vol. 33, no. 1, pp. 54–60, 2016.

[11] I. E. Sommer, C. W. Slotema, Z. J. Daskalakis, E. M. Derks, J. D. Blom, and M. van der Gaag, "The treatment of hallucinations in schizophrenia spectrum disorders," *Schizophrenia Bull.*, vol. 38, no. 4, pp. 704–714, 2012.

[12] S. Ahn et al., "Targeting reduced neural oscillations in patients with schizophrenia by transcranial alternating current stimulation," *Neuroimage*, vol. 186, pp. 126–136, 2019.

[13] M. Zhang, R. B. Force, C. Walker, S. Ahn, L. F. Jarskog, and F. Frohlich, "Alpha transcranial alternating current stimulation reduces depressive symptoms in people with schizophrenia and auditory hallucinations: A double-blind, randomized pilot clinical trial," *Schizophrenia*, vol. 8, no. 1, pp. 1–17, 2022.

[14] C. S. Herrmann, S. Rach, T. Neuling, and D. Strüber, "Transcranial alternating current stimulation: A review of the underlying mechanisms and modulation of cognitive processes," *Front. Hum. Neurosci.*, vol. 7, pp. 1–13, 2013.

[15] M. X. Cohen, "Where does EEG come from and what does it mean?," *Trends Neurosci.*, vol. 40, no. 4, pp. 208–218, 2017.

[16] V. Kumar, V. Shivakumar, H. Chhabra, A. Bose, G. Venkatasubramanian, and B. N. Gangadhar, "Functional near infra-red spectroscopy (fNIRS) in schizophrenia: A review," *Asian J. Psychiatry*, vol. 27, pp. 18–31, 2017.

[17] V. Kumar et al., "Prefrontal cortex activation during working memory task in schizophrenia: A fNIRS study," *Asian J. Psychiatry*, vol. 56, 2021, Art. no. 102507.

[18] A. Aleksandrowicz et al., "Frontal brain activity in individuals at risk for schizophrenic psychosis and bipolar disorder during the emotional stroop task–an fNIRS study," *NeuroImage, Clin.*, vol. 26, 2020, Art. no. 102232.

[19] U. Ghafoor, D. Yang, and K.-S. Hong, "Neuromodulatory effects of HD-tACS/tDCS on the prefrontal cortex: A resting-state fNIRS-EEG study," *IEEE J. Biomed. Health Informat.*, vol. 26, no. 5, pp. 2192–2203, May 2022.

[20] U. Ghafoor, M. A. Khan, D. Yang, and K.-S. Hong, "Influence of tACS/tDCS on resting state effective connectivity in the frontal cortex: An functional near-infrared spectroscopy study," in *Proc. 13th Asian Control Conf.*, 2022, pp. 1563–1568.

[21] D. Yang, M.-K. Kang, G. Huang, A. T. Eggebrecht, and K.-S. Hong, "Repetitive transcranial alternating current stimulation to improve working memory: An EEG-fNIRS study," *IEEE Trans. Neural Syst. Rehabil. Eng.*, vol. 32, pp. 1257–1266, 2024.

[22] E. Başar and B. Güntekin, "Review of delta, theta, alpha, beta, and gamma response oscillations in neuropsychiatric disorders," *Supplements Clin. Neuriophysiol.*, vol. 62, pp. 303–341, 2013.

[23] E. Başar, C. Başar-Eroğlu, B. Güntekin, and G. G. Yener, "Brain's alpha, beta, gamma, delta, and theta oscillations in neuropsychiatric diseases: Proposal for biomarker strategies," *Supplements Clin. Neuriophysiol.*, vol. 62, pp. 19–54, 2013.

[24] Q. Zou, X. Miao, D. Liu, D. J. Wang, Y. Zhuo, and J.-H. Gao, "Reliability comparison of spontaneous brain activities between bold and CBF contrasts in eyes-open and eyes-closed resting states," *Neuroimage*, vol. 121, pp. 91–105, 2015.

[25] Z. Y. Ong, A. Saidatul, and Z. Ibrahim, "Power spectral density analysis for human EEG-based biometric identification," in *Proc. 2018 Int. Conf. Comput. Approach Smart Syst. Des. Appl.*, 2018, pp. 1–6.

[26] M. S. Safi and S. M. M. Safi, "Early detection of Alzheimer's disease from eeg signals using Hjorth parameters," *Biomed. Signal Process. Control*, vol. 65, 2021, Art. no. 102338.

[27] Y. Hirano and P. J. Uhlhaas, "Current findings and perspectives on aberrant neural oscillations in schizophrenia," *Psychiatry Clin. Neurosci.*, vol. 75, no. 12, pp. 358–368, 2021.

[28] S.-H. Oh, Y.-R. Lee, and H.-N. Kim, "A novel EEG feature extraction method using Hjorth parameter," *Int. J. Electron. Elect. Eng.*, vol. 2, no. 2, pp. 106–110, 2014.

[29] T. Cecchin, R. Ranta, L. Koessler, O. Caspary, H. Vespignani, and L. Maillard, "Seizure lateralization in scalp EEG using Hjorth parameters," *Clin. Neuriophysiol.*, vol. 121, no. 3, pp. 290–300, 2010.

[30] G. Sharma, R. Saxena, Y. Kaushal, S. Chandra, V. Singh, and A. Prakash, "Non-linear EEG correlates of route learning in virtual maze," in *Proc. 2016 Int. Conf. Commun. Electron. Syst.*, 2016, pp. 1–6.

[31] S. Liu et al., "Alterations in patients with first-episode depression in the eyes-open and eyes-closed conditions: A resting-state EEG study," *IEEE Trans. Neural Syst. Rehabil. Eng.*, vol. 30, pp. 1019–1029, 2022.

[32] I. Alekseichuk, M. Wischnewski, and A. Opitz, "A minimum effective dose for (transcranial) alternating current stimulation," *Brain Stimul., Basic, Transl., Clin. Res. Neuromodulation*, vol. 15, no. 5, pp. 1221–1222, 2022.

[33] Y. Chang et al., "Temporal hyper-connectivity and frontal hypo-connectivity within gamma band in schizophrenia: A resting state eeg study," *Schizophrenia Res.*, vol. 264, pp. 220–230, 2024.

[34] S. Liu, X. Wang, X. Zhang, Y. Chang, J. Liao, and D. Ming, "Double-blind, randomized, placebo-controlled clinical trial with gamma-band transcranial alternating current stimulation for the treatment of schizophrenic auditory hallucinations," *Res. Square*, to be published. [Online]. Available: https://doi.org/10.21203/rs.3.rs-3162173/v1

[35] S. Blum, N. S. Jacobsen, M. G. Bleichner, and S. Debener, "A Riemannian modification of artifact subspace reconstruction for EEG artifact handling," *Front. Hum. Neurosci.*, vol. 13, pp. 1–10, 2019.

[36] L. Pion-Tonachini, K. Kreutz-Delgado, and S. Makeig, "ICLabel: An automated electroencephalographic independent component classifier, dataset, and website," *NeuroImage*, vol. 198, pp. 181–197, 2019.

[37] A. Ahmadi, A. Khorasani, V. Shalchyan, and M. R. Daliri, "State-based decoding of force signals from multi-channel local field potentials," *IEEE Access*, vol. 8, pp. 159089–159099, 2020.

[38] P. Welch, "The use of fast Fourier transform for the estimation of power spectra: A method based on time averaging over short, modified periodograms," *IEEE Trans. Audio Electroacoustics*, vol. TAU-15, no. 2, pp. 70–73, Jun. 1967.

[39] A. Ameera, A. Saidatul, and Z. Ibrahim, "Analysis of EEG spectrum bands using power spectral density for pleasure and displeasure state," *IOP Conf. Ser., Mater. Sci. Eng.*, vol. 557, no. 1, 2019, Art. no. 012030.

[40] S. Noshadi, V. Abootalebi, M. T. Sadeghi, and M. S. Shahvazian, "Selection of an efficient feature space for eeg-based mental task discrimination," *Biocybernetics Biomed. Eng.*, vol. 34, no. 3, pp. 159–168, 2014.

[41] T. H. Nayani and A. S. David, "The auditory hallucination: A phenomenological survey," *Psychol. Med.*, vol. 26, no. 1, pp. 177–189, 1996.

[42] M. A. Albrecht, G. Roberts, G. Price, J. Lee, R. Iyyalol, and M. T. Martin-Iverson, "The effects of dexamphetamine on the resting-state electroencephalogram and functional connectivity," *Hum. Brain Mapping*, vol. 37, no. 2, pp. 570–588, 2016.

[43] B. Hjorth, "EEG analysis based on time domain properties," *Electroencephalogr. Clin. Neuriophysiol.*, vol. 29, no. 3, pp. 306–310, 1970.

[44] J. R. de Miras, A. Ibáñez-Molina, M. Soriano, and S. Iglesias-Parro, "Schizophrenia classification using machine learning on resting state EEG signal," *Biomed. Signal Process. Control*, vol. 79, 2023, Art. no. 104233.

[45] X. Liu et al., "Altered gamma oscillations and beta–gamma coupling in drug-naive first-episode major depressive disorder: Association with sleep and cognitive disturbance," *J. Affect. Disord.*, vol. 316, pp. 99–108, 2022.

[46] C. R. Genovese, N. A. Lazar, and T. Nichols, "Thresholding of statistical maps in functional neuroimaging using the false discovery rate," *Neuroimage*, vol. 15, no. 4, pp. 870–878, 2002.

[47] S. Liu et al., "3DCANN: A spatio-temporal convolution attention neural network for EEG emotion recognition," *IEEE J. Biomed. Health Informat.*, vol. 26, no. 11, pp. 5321–5331, Nov. 2022.

[48] J. Cheng et al., "Emotion recognition from multi-channel EEG via deep forest," *IEEE J. Biomed. Health Informat.*, vol. 25, no. 2, pp. 453–464, Feb. 2021.

[49] T. Zhang, W. Zheng, Z. Cui, Y. Zong, and Y. Li, "Spatial–temporal recurrent neural network for emotion recognition," *IEEE Trans. Cybern.*, vol. 49, no. 3, pp. 839–847, Mar. 2019.
[50] M. A. L. Hema, "Development of denoising methodologies for enhancement of sensitivity in radiographic images," *Int. J. Adv. Res. Elect., Electronics Instrum. Energy*, vol. 3, pp. 222–227, 2014.
[51] C.-C. Chang and C.-J. Lin, "LIBSVM: A library for support vector machines," *ACM Trans. Intell. Syst. Technol.*, vol. 2, no. 3, pp. 1–27, 2011.
[52] A. Liaw et al., "Classification and regression by randomforest," *R News*, vol. 2, no. 3, pp. 18–22, 2002.
[53] K. Madsen, H. B. Nielsen, and O. Tingleff, "Methods for non-linear least squares problems," *Inform. Math. Modelling*, Tech. Univ. Denmark, Apr. 2004.
[54] T. Wang et al., "A novel gait analysis method based on the pseudo-velocity model for depression detection," in *Proc. 2020 IEEE Int. Conf. E-Health Netw., Appl. Serv.*, 2021, pp. 1–6.
[55] T. Wang et al., "A gait assessment framework for depression detection using kinect sensors," *IEEE Sensors J.*, vol. 21, no. 3, pp. 3260–3270, Feb. 2021.
[56] R. P. Bentall, "The illusion of reality: A review and integration of psychological research on hallucinations," *Psychol. Bull.*, vol. 107, no. 1, pp. 82–95, 1990.
[57] P. Allen et al., "Neuroimaging auditory hallucinations in schizophrenia: From neuroanatomy to neurochemistry and beyond," *Schizophrenia Bull.*, vol. 38, no. 4, pp. 695–703, 2012.
[58] D. A. Silbersweig et al., "A functional neuroanatomy of hallucinations in schizophrenia," *Nature*, vol. 378, no. 6553, pp. 176–179, 1995.
[59] B. R. Lennox, S. B. G. Park, I. Medley, P. G. Morris, and P. B. Jones, "The functional anatomy of auditory hallucinations in schizophrenia," *Psychiatry Res., Neuroimag.*, vol. 100, no. 1, pp. 13–20, 2000.
[60] P. Woodruff et al., "Auditory hallucinations and perception of external speech," *Lancet*, vol. 346, no. 8981, pp. 1035–1036, 1995.
[61] A. Vercammen, H. Knegtering, J. A. den Boer, E. J. Liemburg, and A. Aleman, "Auditory hallucinations in schizophrenia are associated with reduced functional connectivity of the temporo-parietal area," *Biol. Psychiatry*, vol. 67, no. 10, pp. 912–918, 2010.
[62] S. M. Lawrie, C. Buechel, H. C. Whalley, C. D. Frith, K. J. Friston, and E. C. Johnstone, "Reduced frontotemporal functional connectivity in schizophrenia associated with auditory hallucinations," *Biol. Psychiatry*, vol. 51, no. 12, pp. 1008–1011, 2002.
[63] K. M. Spencer, M. A. Niznikiewicz, P. G. Nestor, M. E. Shenton, and R. W. McCarley, "Left auditory cortex gamma synchronization and auditory hallucination symptoms in schizophrenia," *BMC Neurosci.*, vol. 10, pp. 1–13, 2009.
[64] C. Mulert, V. Kirsch, R. Pascual-Marqui, R. W. McCarley, and K. M. Spencer, "Long-range synchrony of gamma oscillations and auditory hallucination symptoms in schizophrenia," *Int. J. Psychophysiol.*, vol. 79, no. 1, pp. 55–63, 2011.
[65] S. Steinmann, G. Leicht, C. Andreou, N. Polomac, and C. Mulert, "Auditory verbal hallucinations related to altered long-range synchrony of gamma-band oscillations," *Sci. Rep.*, vol. 7, no. 1, 2017, Art. no. 8401.
[66] S.-H. Lee, J.-S. Choo, W.-Y. Im, and J.-H. Chae, "Nonlinear analysis of electroencephalogram in schizophrenia patients with persistent auditory hallucination," *Psychiatry Investigation*, vol. 5, no. 2, pp. 115–120, 2008.
[67] R. L. Mitchell and T. J. Crow, "Right hemisphere language functions and schizophrenia: The forgotten hemisphere?," *Brain*, vol. 128, no. 5, pp. 963–978, 2005.
[68] B. Min et al., "Prediction of individual responses to electroconvulsive therapy in patients with schizophrenia: Machine learning analysis of resting-state electroencephalography," *Schizophrenia Res.*, vol. 216, pp. 147–153, 2020.
[69] R. Redlich et al., "Prediction of individual response to electroconvulsive therapy via machine learning on structural magnetic resonance imaging data," *JAMA Psychiatry*, vol. 73, no. 6, pp. 557–564, 2016.
[70] B. Cao et al., "Treatment response prediction and individualized identification of first-episode drug-naive schizophrenia using brain functional connectivity," *Mol. Psychiatry*, vol. 25, no. 4, pp. 906–913, 2020.